Dynamic Flood Routing with Explicit and Implicit Numerical Solution Schemes

By Ming Jin[1] and D. L. Fread,[2] Member, ASCE

Abstract: A characteristics-based, upwind, explicit numerical scheme is developed for one-dimensional (1D) unsteady flow modeling of natural rivers and implemented into the U.S. National Weather Service (NWS) FLDWAV model in combination with the original four-point implicit scheme. The new explicit scheme is extensively tested and compared with the implicit scheme. The study shows that the new explicit scheme provides improved versatility and accuracy in some situations, such as particularly large dam-break waves and other unsteady flows with near critical mixed-flow regimes. A technique for implicit-explicit multiple routing is introduced to incorporate the advantages of using both schemes within an application of the FLDWAV model.

INTRODUCTION

Channel flood routing has long been of vital concern as we have sought to predict the characteristics of flood waves. Mathematical techniques to predict channel flood wave propagation have continually been developed, and many channel-routing models have been proposed. Among the various channel-routing models, those based on the complete one-dimensional (1D) hydrodynamic (Saint-Venant) equations have found increasing applications.

The U.S. National Weather Service (NWS) has been developing a generalized channel flood-routing model, FLDWAV (Fread 1985, 1993) to replace the popular dynamic DAMBRK and DWOPER models (Fread 1977, 1978, 1988; Chow et al. 1988). More model capability has been added to the FLDWAV model, including a Kalman filter estimator for real-time updating using on-line observations (Fread and Jin 1993). A recent enhancement to the FLDWAV model is the addition of a characteristics-based, upwind, explicit solution scheme for the Saint-Venant equations; this has been incorporated into the FLDWAV model via an implicit-explicit multiple dynamic-routing technique.

The original numerical scheme used for dynamic routing in FLDWAV is based on the four-point, implicit, nonlinear finite-difference solution of the Saint-Venant equations. The implicit scheme has flexible requirements for selection of the computational time steps and distance intervals, which have been proven to be very efficient, and excellent numerical stability and reliability in numerous unsteady flow modeling applications through many years of use.

The four-point implicit scheme was found to have numerical stability problems when the flow changed from subcritical to supercritical flow or conversely (mixed-flow regime). A mixed-flow technique was developed to enable the four-point implicit scheme to successfully treat many situations of such mixed-flow conditions (Fread 1983, 1985). This technique involved locating the control points where critical flow occurs, dividing the entire routing reach at each time step into a series of subcritical and supercritical subreaches, and computing each subreach separately using appropriate external and internal boundary conditions along with appropriate subcritical or supercritical solution algorithms. In this technique, the correct numerical characteristics transmission direction is maintained in the solution procedure in which the supercritical flows are solved in a downstream marching direction while subcritical flows are solved by a double sweeping process (upstream to downstream followed by downstream to upstream). The latter is inherent in the efficient (computational time and storage) matrix solution technique (Fread 1971) used in FLDWAV. This technique works well when control points are easy to define and locate, such as the point where channel slope changes abruptly from subcritical to supercritical or conversely, or when the Froude number has a large change upstream and downstream of the point, at which an apparent hydraulic jump would occur.

In many mixed-flow situations, the flow can be near critical, or either slightly above or below critical throughout a channel reach; in this case, it is not easy to locate the critical control point that moves as the flow rate changes. This causes the four-point implicit scheme, with the mixed-flow technique, to have numerical stability and accuracy problems when modeling such mixed flows, with near critical state, where the Froude number remains both temporally and spatially between about 0.9 and 1.1.

Also, it was observed that the four-point implicit scheme, with the mixed-flow technique, has difficulties when solving the Saint-Venant equations for an instantaneous, or near-instantaneous, very large dam-break–induced flood wave, which produces a moving supercritical-subcritical mixed-flow interface.

In the literature, some techniques have been proposed to deal with unsteady flows having strong shocks or mixed-flow regimes such as: the Godunov method (Savic and Holly 1993); the ENO explicit scheme (Yang et al. 1993); the TVD-McCormack scheme (Nakatani and Komura 1993); the McCormack, Lambda, and Gabutti schemes (Fennema and Chaudhry 1986); the Beam and Warming scheme (Fennema and Chaudhry 1987); and the flux difference schemes (Jha et al. 1995). Although these techniques provide numerical tools for open-channel flows with strong shocks resulting from an instantaneous dam break, all of them were proposed for only prismatic or rectangular nonprismatic channels, which are not representative of natural rivers.

The explicit scheme presented herein has the capability of not only effectively modeling flows with strong shocks (near instantaneous dam-break waves) or subcritical/supercritical mixed flows, but also dealing with natural river properties such as nonprismatic cross sections, off-channel storage, channel cross sections with wide floodplains, various internal boundaries such as dams and bridges, abrupt contractions or expansions of cross sections, and so on.

The new scheme also has the capability of coping with a variety of external boundary conditions, such as stage or discharge hydrographs, or rating curves defining single or looped

[1]Visiting Sci., Hydrologic Res. Lab., Nat. Weather Service, NOAA, 1325 East-West Highway, Silver Spring, MD 20910.
[2]Dir., Ofc. of Hydro., Nat. Weather Service, NOAA, 1325 East-West Highway, Silver Spring, MD.

Note. Discussion open until August 1, 1997. To extend the closing date one month, a written request must be filed with the ASCE Manager of Journals. The manuscript for this paper was submitted for review and possible publication on May 22, 1995. This paper is part of the ***Journal of Hydraulic Engineering***, Vol. 123, No. 3, March, 1997. ©ASCE, ISSN 0733-9429/97/0003-0166–0173/$4.00 + $.50 per page. Paper No. 10777.

stage-discharge relations, so that it can be easily incorporated to model special mixed flows simultaneously in an application which uses the four-point implicit scheme within the FLDWAV model.

Unlike most spatially symmetric schemes, an upwind scheme is based on the local characteristic direction and thus always ensures the correct characteristic direction. Also, the total variation diminishing feature of an upwind scheme makes it a favorable choice for modeling waves with strong shocks.

In this study, a characteristics-based, upwind, explicit scheme for the conservation form of the complete Saint-Venant equations for nonprismatic channels is constructed, extensively tested, compared with the four-point implicit scheme, and implemented into the FLDWAV model as an additional available numerical solution scheme.

Also, a technique for explicit-implicit multiple routing has been developed so that one can take advantage of these two numerical schemes and apply them to different subreaches of an entire routing reach. This enhancement to the FLDWAV model is reported herein.

MODEL FORMULATION

Governing Equations

The Saint-Venant equations of 1D unsteady flow in nonprismatic channels are the basic equations used in the FLDWAV model, i.e.

$$\frac{\partial Q}{\partial x} + \frac{\partial (A + A_o)}{\partial t} - q = 0 \tag{1}$$

$$\frac{\partial Q}{\partial t} + \frac{\partial (Q^2/A)}{\partial x} + gA\left(\frac{\partial h}{\partial x} + S_f + S_e\right) + L + W_f B = 0 \tag{2}$$

where

$$S_f = \frac{n^2 |Q| Q}{\lambda A^2 R^{4/3}} = \frac{|Q| Q}{K_c^2}; \quad S_e = \frac{K_e \partial (Q/A)^2}{2g \partial x}; \quad W_f = C_w |V_r| V_r \tag{3}$$

where x = distance along the longitudinal axis of the channel; t = time; Q = discharge; A = active cross-sectional area; A_o = inactive (off-channel storage) cross-sectional area; q = lateral inflow; g = gravity constant; h = water-surface elevation; B = wetted top width of the cross section; L = momentum effect of lateral flow ($L = -qv_x$, where v_x = velocity of the lateral inflow in the x-direction of the channel flow); S_f = friction slope due to the bed resistance; n = Manning n; R = hydraulic radius approximated by (A/B); K_c = channel conveyance factor; λ = system of units coefficient associated with the Manning equation to determine the resistance slope ($\lambda = 1$ for the metric system, and $\lambda = 2.21$ for the English system); S_e = local loss slope; K_e = expansion (negative) or contraction (positive) coefficient; W_f = wind term representing the resistance effect of wind on the water surface; C_w = nondimensional wind coefficient; and the wind velocity relative to the water is $V_r = V_w \cos w + V$, where V_w = velocity of wind, w = azimuth angle the wind direction makes with the x-axis, and V = velocity of the unsteady flow.

To construct a characteristics-based, upwind, explicit scheme, the basic equations are transformed into the conservation form of mass and momentum expressed in vector notation for convenience, i.e.

$$\frac{\partial \mathbf{U}}{\partial t} + \frac{\partial \mathbf{F(U)}}{\partial x} + \mathbf{S(U)} = 0 \tag{4}$$

or

$$\frac{\partial \mathbf{U}}{\partial t} + \mathbf{G(U)} \frac{\partial \mathbf{U}}{\partial x} + \mathbf{S(U)} = 0 \tag{5}$$

where

$$\mathbf{U}(x, t) = \begin{bmatrix} A + A_o \\ Q \end{bmatrix}; \quad \mathbf{G(U)} = \begin{bmatrix} 0 & 1 \\ -\frac{Q^2}{A^2} + \frac{gA}{B} & \frac{2Q}{A} \end{bmatrix} \tag{6}$$

$$\mathbf{F(U)} = \begin{bmatrix} Q \\ \frac{Q^2}{A} + P_1 \end{bmatrix}; \quad \mathbf{S(U)} = \begin{bmatrix} -q \\ gA(S_f + S_e) - P_2 + L + W_f B \end{bmatrix} \tag{7}$$

where

$$P_1 = g \int_{h_b}^{h} A(x, \xi)\, d\xi; \quad P_2 = g \int_{h_b}^{h} \frac{\partial A(x, \xi)}{\partial x}\, d\xi \tag{8}$$

where h_b = elevation of the channel bed at location x; and ξ = dummy variable for the integration. The components of the state variable, $\mathbf{U}(x, t)$, in the conservation form of the basic equations, are now $(A + A_o)$ and Q, and the most useful variable is water-surface elevation h. However, it is easy to obtain h from the numerical solutions of $(A + A_o)$, according to the cross-sectional data of tabular values of channel wetted active and inactive top widths versus water-surface elevation. Also, the state variable integral functions, P_1 and P_2 in (7) can be easily determined during the computations by a reverse table look-up algorithm.

Numerical Scheme Formulation

Since the principle of an upwind, explicit scheme is to use a one-sided, finite-difference approximation for the space derivative, according to the time-dependent local characteristic direction (eigenvalues or local characteristic velocity) similar to the derivations of Yang et al. (1993), the flux in (5) is split into two parts with each corresponding to a local characteristic direction. This can be done by splitting the Jacobian vector, $\mathbf{G(U)}$, into two parts in terms of a split normalized Jacobian matrix, i.e.

$$\mathbf{G(U)} = [(\hat{G})^+ + (\hat{G})^-]\mathbf{G(U)} \tag{9}$$

where the split normalized Jacobian matrix is defined by the following:

$$\hat{G}^{\pm} = \begin{bmatrix} -\frac{v}{c}\left(\frac{\hat{\lambda}_1^{\pm} - \hat{\lambda}_2^{\pm}}{2}\right) + \left(\frac{\hat{\lambda}_1^{\pm} + \hat{\lambda}_2^{\pm}}{2}\right) & \frac{1}{c}\left(\frac{\hat{\lambda}_1^{\pm} - \hat{\lambda}_2^{\pm}}{2}\right) \\ \frac{(c^2 - v^2)}{c}\frac{(\hat{\lambda}_1^{\pm} - \hat{\lambda}_2^{\pm})}{2} & \frac{v}{c}\left(\frac{\hat{\lambda}_1^{\pm} - \hat{\lambda}_2^{\pm}}{2}\right) + \left(\frac{\hat{\lambda}_1^{\pm} + \hat{\lambda}_2^{\pm}}{2}\right) \end{bmatrix} \tag{10}$$

and

$$\lambda_i = \frac{Q}{A} \pm \sqrt{\frac{gA}{B}} = v \pm c; \quad \hat{\lambda}_i^{\pm} = \frac{1}{2}(1 \pm \text{sgn}\, \lambda_i), \ (i = 1, 2) \tag{11}$$

where $i = 1$ for $v + c$, and $i = 2$ for $v - c$; v = local cross-sectional average velocity, and c = local dynamic wave velocity; and the term (sgn) is the sign function. The flux in (5) can thus be split, i.e.

$$\frac{\partial \mathbf{U}}{\partial t} + (\hat{G}^+ + \hat{G}^-)\frac{\partial \mathbf{F(U)}}{\partial x} + \mathbf{S(U)} = 0 \tag{12}$$

An upwind, explicit scheme for (12) can be constructed in which the subscript (j) refers to the computational cross-sectional (node) number, and the subscript (n) refers to a point on the time line, i.e.

$$\frac{\mathbf{U}_j^{n+1} - \mathbf{U}_j^n}{\Delta t} + (\hat{G}^+)_{j-1/2}^n \frac{\mathbf{F}(\mathbf{U}_j^n) - \mathbf{F}(\mathbf{U}_{j-1}^n)}{\Delta x_{j-1,j}}$$

$$+ (\hat{G}^-)_{j+1/2}^n \frac{\mathbf{F}(\mathbf{U}_{j+1}^n) - \mathbf{F}(\mathbf{U}_j^n)}{\Delta x_{j,j+1}} + \mathbf{S}(\mathbf{U}_j^n) = 0 \tag{13}$$

where values of the state variable, $\mathbf{U}(x, t)$, are known at all computational nodes at time t^n; and values of $\mathbf{U}(x, t)$ for all interior nodes at time t^{n+1} can be directly obtained from it.

Boundary Conditions

Most explicit schemes use the method of characteristics to treat external boundary conditions. Although this method is efficient when treating channels of rectangular cross sections, it is not as efficient when dealing with complicated nonprismatic channels or channels with off-channel storage.

A technique has been developed to treat both external and internal boundary conditions more effectively. An external boundary, such as a known stage or discharge hydrograph for the upstream and downstream boundaries, or a known relationship between stage and discharge, such as a single or looped rating curve for the downstream boundary condition, is specified at the most upstream cross section and at the most downstream cross section. Internal boundaries are used for dams or bridges. All values of the state variable, $\mathbf{U}(x, t)$, can be determined if another equation is provided for each boundary and solved in connection with the specified boundary condition.

In this study, the extra equation for both external boundaries, or for the internal boundaries, is derived by integrating (1) for the first ($i = 1$) and last ($i = N - 1$) computational time and distance steps as

$$\int_{t^n}^{t^{n+1}} \int_{x_i}^{x_{i+1}} \left[\frac{\partial Q}{\partial x} + \frac{\partial (A + A_0)}{\partial t} - q \right] dx\, dt = 0 \tag{14}$$

or

$$\Delta t(\bar{Q}_{i+1} - \bar{Q}_i) + \Delta x[\underline{(A + A_0)}^{n+1} - \underline{(A + A_0)}^n] - 2\bar{q}\Delta x \Delta t = 0 \tag{15}$$

where $i = 1$ for the upstream boundary, and $i = N - 1$ for the downstream boundary (N = total number of computational cross sections); the bar stands for a temporal averaging, and the underline stands for a spatial averaging, i.e., $\underline{(A + A_0)} = 0.5[(A + A_0)_i + (A + A_0)_{i+1}]$, $\bar{Q} = 0.5(Q^n + Q^{n+1})$; and $\bar{q}$ = time-averaged lateral inflow or outflow within the computational distance step.

Also, (15) can be applied to upstream and downstream reaches of a hydraulic structure (internal boundary such as dam or bridge), together with an appropriate internal boundary equation (such as weir equation) representing the relationship between flow through the structure and water-surface elevations both upstream and downstream of the structure.

A comparison of the upwind solutions, using (15), with implicit solutions for numerous cases has shown that this method of treating boundary conditions works well for a variety of external and internal boundaries.

Selection of Computational Δt and Δx

Unlike unconditionally stable implicit schemes, most explicit schemes are restricted to the Courant-Friedrich-Lewy (CFL) condition for numerical stability. For the upwind scheme presented herein, the CFL condition can be written as follows:

$$\Delta t \le C_n \min \left(\frac{\Delta x}{v + c} \right)_i, \quad (C_n \le 1.0) \tag{16}$$

where C_n = Courant number. A large value of C_n (0.9–1 can be used for simple prismatic channels. Value C_n has to reduced for complicated channel geometry such as rapid e pansions and contractions, rapid changes in slope, chan cross sections with wide floodplains, or a large portion of o channel storage due to an increased effect of the source te $\mathbf{S}(\mathbf{U}_j^n)$ in (13). In the FLDWAV model, options are provid to input either Δt or C_n.

After many years of experience with the selection of co putational distance step values for the NWS implicit dynan routing models in numerous applications, and more recen supported by a theoretical derivation (Fread and Lewis 199 a criteria for Δx is recommended as follows:

$$\Delta x \le C_b \frac{T_r}{M} \tag{1}$$

where T_r = hydrograph's time of rise (time from the significa beginning of increased discharge to the peak of the dischar hydrograph) in hours; C_b = bulk wave speed (the celerity a sociated with an essential characteristic of the unsteady flo such as the peak or center of gravity of the hydrograph) in n h; and M = function of the flow properties and generally vari between about 8 and 40 (a value of about 20 for M has prov to be generally acceptable).

Extensive testing in this study has shown that smaller co putational distance steps for the upwind, explicit scheme a needed to match the same accuracy as that of the implic scheme. Therefore, a somewhat larger value of M (30–40) recommended for the reaches where the explicit scheme used.

TESTING EXAMPLES

Example 1—Idealized Dam-Break Problem

To examine the performance of the upwind, explicit schem presented herein, an idealized dam-break problem that has a analytical solution is solved with the upwind, explicit schem these results are compared with those of the analytical solu tion. A dam in a wide, horizontal, rectangular, and frictionles channel, with still water at constant depths of 12.1 and 0.6 m, upstream and downstream of the dam, respectively is in stantaneously removed across its entire width at the beginnin of the computation ($t = 0.0$). The analytical solution is ob tained by using Stoker's method (Stoker 1957).

Fig. 1 compares the computed water-surface profile fro the analytical and upwind, explicit numerical solutions for th time $t = 10$ s after the removal of the dam. This problem

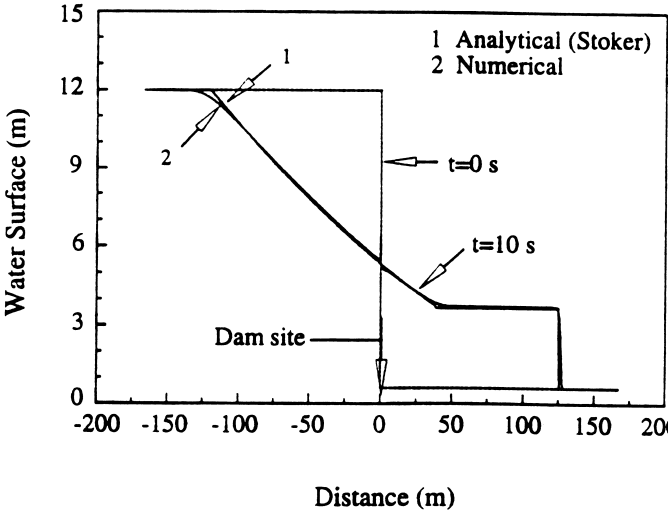

FIG. 1. Stoker Dam-Break Problem ($t = 10$ s)

characterized by a sudden formation of a bore, or sharp wavefront, that travels downstream. The upwind, explicit scheme was also tested for different initial depth ratios (tailwater depth to the reservoir depth) ranging from 0.05, as shown in Fig. 1, to a value as small as 0.000025. The computational results compare closely with the analytical results, both upstream of the dam (negative wave region) and downstream in the bore region where an insignificant computational smoothing of the bore front occurs.

Example 2—Large Dam-Break Waves

In this example, a 36.6 m high dam is located at 11.3 km of a 32.2 km routing reach. The channel has irregular and nonprismatic cross sections at 0, 8.05, 11.3, 16.1, 24.1, and 32.2 km, and the bed slope changes from 0.0042 upstream of the dam to 0.0019 downstream of the dam. A constant Manning n of 0.04 is used. The dam fails, and the resulting dam-break peak discharge and wave shape depend on the time of failure (T_f) of the dam, the breach shape and dimensions, and inflow into the reservoir. The time of failure is defined herein as the time from the beginning of the formation of the breach until the final formation of the specified breach size is attained. It is assumed that the breach has the same shape as the nearly trapezoidal cross section of the dam at time T_f. Also, there is a small constant upstream inflow of 142 m^3/s into the reservoir (upstream boundary condition). The time of failure is an important parameter for the dam-break outflow and the resulting dam failure flood wave. In both the implicit and explicit solution schemes, the breached dam is treated as an internal boundary within the entire 32.2 km dynamic routing reach.

It is found that for a time of failure of about 0.05 h or larger, both explicit and implicit methods get approximately the same computational results. The computed attenuation of peak discharge and peak stage elevation along the channel for T_f = 0.05 h are shown in Figs. 2(a) and 2(b). Nonprismatic effects cause irregularities in the peak stage profiles at 16.1 and 24.1 km. The computed hydrographs at the dam site from the explicit and implicit schemes are compared in Fig. 2(c). Variable computational distance steps are used; these change from 0.5 to 0.3 km upstream of the dam and from 0.03 to 0.16 km downstream of the dam, respectively. The time step used is 0.0025 h for the explicit solution scheme and 0.001 h for the implicit scheme.

For this example the implicit scheme experienced nonconvergence problems when the time of failure was less than 0.05 h. This was due to a type of mixed flow in which a supercritical/subcritical interface develops spontaneously below the dam and progresses downstream. The formation of the supercritical regime was produced by an increase in the dam failure peak outflow. The outflow increase was, in turn, caused by the decrease in the time of failure (T_f), which reduces the extent that the reservoir level decreases as the breach forms and the breach outflow begins to drain the reservoir. The resulting higher reservoir elevation when the breach reaches its final and largest size produces a greater breach (weir-type) outflow than for the former example with a T_f = 0.05 h. The initiation of supercritical flow associated with the increased breach outflow could also have resulted by increasing the bottom slope of the channel downstream of the dam, reducing the Manning n in the downstream channel, increasing the height of the original reservoir level, and/or increasing the width of the dam breach.

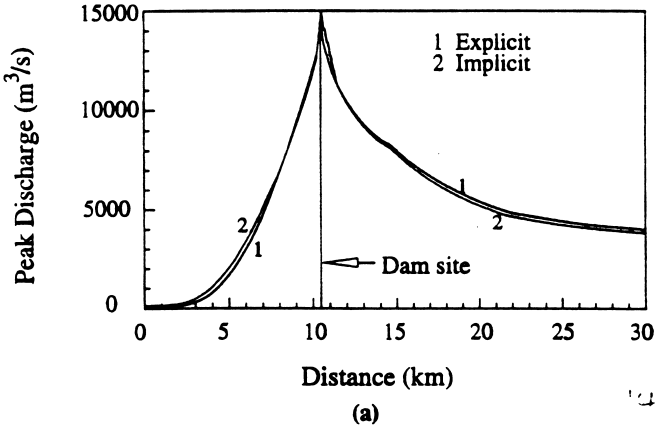

FIG. 2(a). Peak Discharge (Time of Failure = 0.05 h)

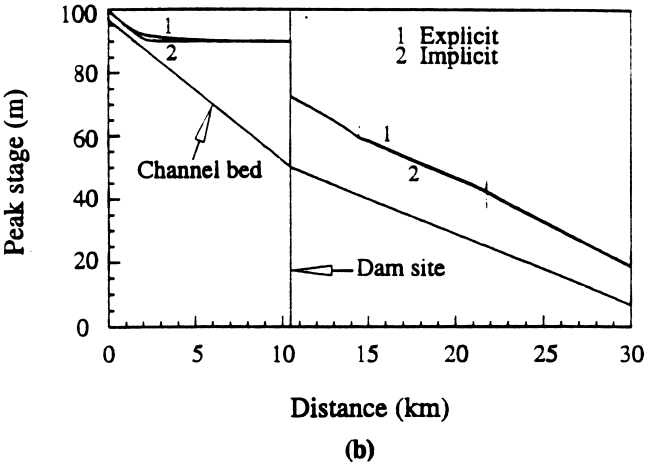

FIG. 2(b). Peak Stage (Time of Failure = 0.05 h)

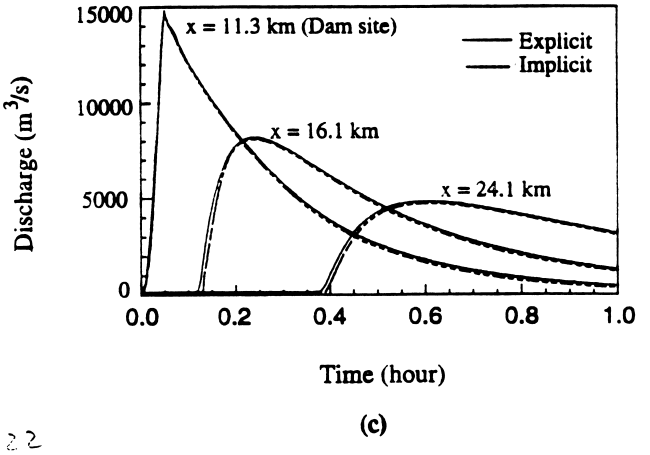

FIG. 2(c). Hydrographs (Time of Failure = 0.05 h)

The four-point implicit scheme with the mixed-flow technique (Fread 1985) is not capable of modeling this type of mixed flow with a moving supercritical/subcritical interface, whereas the characteristics-based, upwind, explicit scheme is capable of modeling such flows.

Results of the explicit scheme applied to a near instantaneous dam-break (T_f = 0.02 h) simulation for the same example previously described are shown in Figs. 3(a)–3(c). Profiles of the computed Froude number along the downstream channel at times t = 0.02, 0.05, 0.10, 0.15, and 0.20 h are shown in Fig. 3(a). The moving supercritical/subcritical interface is shown in each profile for the times 0.02, 0.05, and 0.10. The flow becomes subcritical throughout the entire reach after about t = 0.15 h. The computed water-surface profiles at these five times are shown in Fig. 3(b). The irregularities at 16.1 km in the profiles are caused by the nonprismatic effects. The computed discharge hydrographs at five locations along the channel are shown in Fig. 3(c).

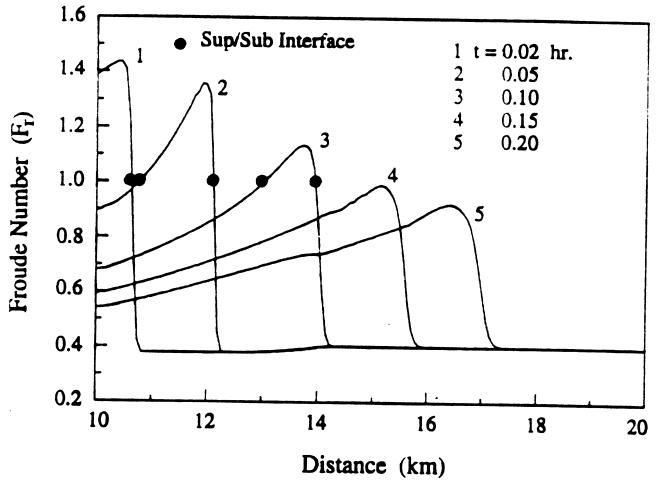

(a)

FIG. 3(a). Froude Number Profiles (T_r = 0.02 h)

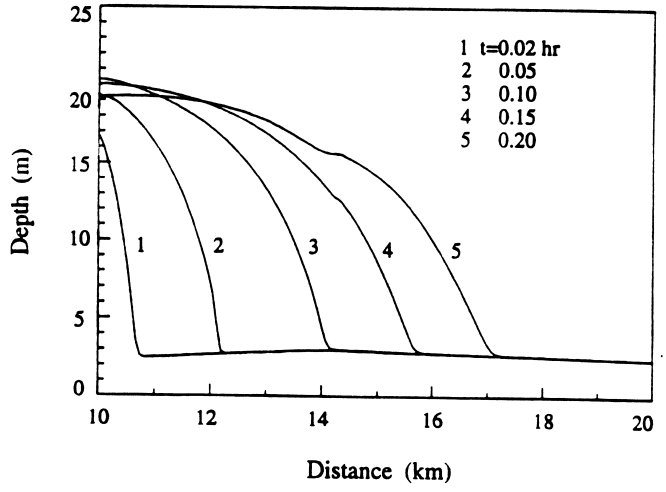

(b)

FIG. 3(b). Water-Depth Profiles (T_r = 0.02 h)

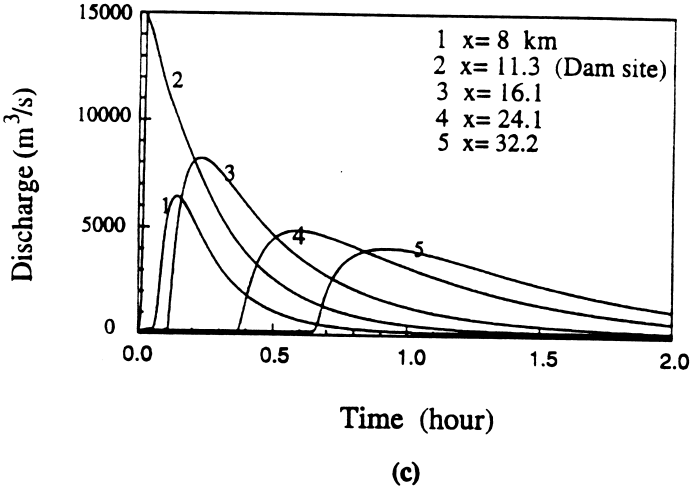

(c)

FIG. 3(c). Discharge Hydrograph (T_r = 0.02 h)

Example 3—Near Critical Mixed-Flow Regimes

In this example, a flood wave is routed through a 48.3 km reach of a rectangular channel with a width of 61 m and a slope of 0.0076. This situation simulates an unsteady flow in a channel with near critical slope. The upstream boundary condition is a specified discharge hydrograph with an initial discharge of 71 m^3/s and a peak discharge of 1,415 m^3/s. A linear increase of the discharge from the initial flow to the peak is used with a time of rise (T_r) of 0.4 h, and linear recession from the peak to the initial flow within 0.4 h is also used. A free-flow condition is specified as the downstream boundary condition (a loop rating will be generated automatically in the FLDWAV model under a free-flow condition). This example is designed to test the performance of the upwind, explicit scheme for the case of near critical mixed flow along the routing reach.

Three different unsteady flow situations are observed by changing the Manning n. A subcritical flow is obtained using a Manning n of 0.035, and a supercritical flow is obtained using a Manning n of 0.025. When a Manning n of 0.03 is used, a complicated mixed-flow situation occurs in which a supercritical flow region is associated with only the flood peak, and this region moves as the flood peak travels downstream while upstream and downstream of this region the flows are subcritical.

Fig. 4(a) presents the computed peak discharge profiles from both the implicit and the explicit schemes. Similar numerical results are obtained from the two schemes for the supercritical and subcritical flow situations, as shown by the two profiles for the subcritical and supercritical flows in Fig. 4(a). For the mixed-flow situation, a reasonable predicted peak profile from the explicit scheme falls between those of supercritical and subcritical situations, and the implicit scheme produces an un-

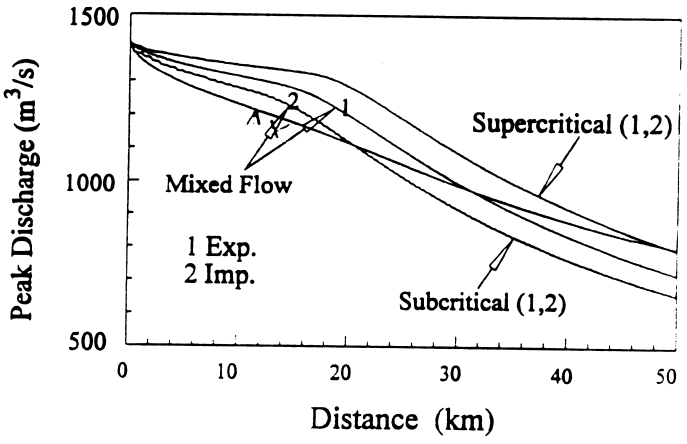

(a)

FIG. 4(a). Peak Discharge Profiles

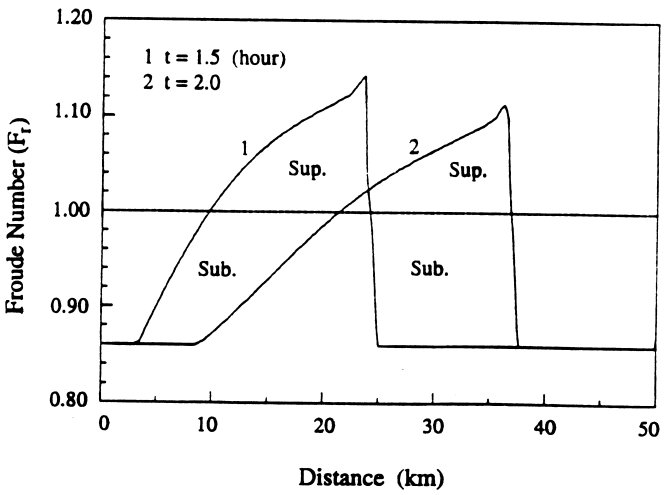

(b)

FIG. 4(b). Froude Number Distributions

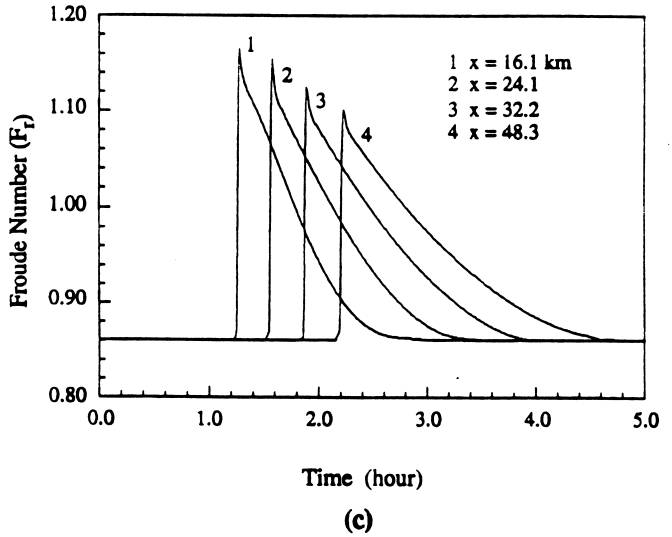

(c)

FIG. 4(c). Froude Number Variation with Time

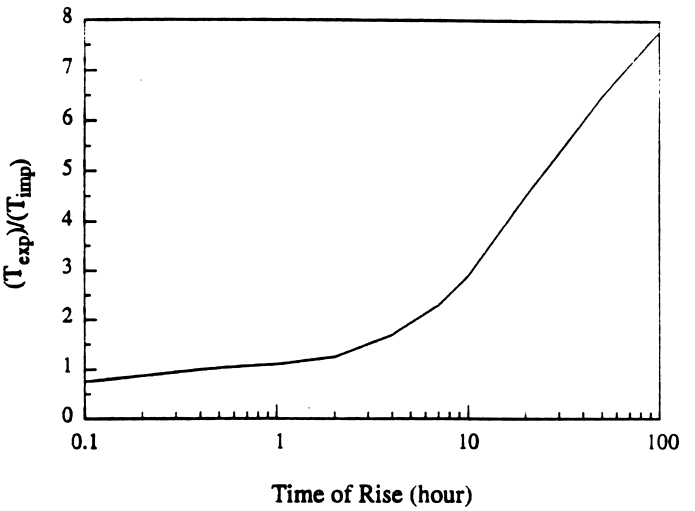

FIG. 5. Ratio of Required Computation Time for Implicit and Explicit Schemes

reasonable peak profile that is lower than that of subcritical flow in the first 19.3 km of the reach.

Fig. 4(b) shows the spatial distribution of the Froude number along the channel at two different times (t = 1.5 and 2.0 h), computed by the explicit scheme for the mixed-flow situation. It is seen that the Froude number changes from about 0.86 (subcritical) to 1.15 (supercritical) at the flood-wave peak; the location of the supercritical portion of the flow moves as the flood peak moves downstream.

In Fig. 4(c), changes of the Froude number with time at locations x = 16.1, 24.1, 32.2, and 48.3 km are shown; the flow regimes at these cross sections can be observed to change from subcritical to supercritical and back to subcritical again as the flood peak passes. Tests of several other mixed-flow cases also show that the upwind, explicit, numerical scheme is capable of modeling the near critical mixed flows or mixed flows with moving subcritical/supercritical regimes.

IMPLICIT-EXPLICIT MULTIPLE ROUTING

Because the numerical stability requirement of the explicit scheme restricts the time step to a Courant condition, the explicit scheme requires smaller computational time steps than the implicit scheme, which is unconditionally stable; therefore, for most applications it requires more computational time. In Fig. 5, the ratio of computational time of the explicit scheme to the computational time of the implicit scheme is plotted as a function of the routed hydrograph's time of rise (T_r). It can be seen that the explicit scheme needs much more computation time when modeling slowly rising flood waves, while it is equally or more time efficient, as the implicit scheme, for very fast-rising waves of about 0.5 h time of rise or smaller. Since fast-rising waves tend to attenuate quickly and the time of rise of a wave increases when it travels downstream, use of the explicit scheme for an entire routing reach may often result in very large computational times. In addition, it has been found in tests for a wide variety of simulations, that the explicit scheme is inferior compared with the implicit scheme regarding the numerical accuracy, especially when modeling the flows in a channel with very nonprismatic features, large change of slopes, cross sections having large portions of dead storage, an abrupt change in computational distance step (over two times for adjacent cross sections), and so on. This is caused by an increased effect of the terms P_1 and P_2 in (8) and the source term S(U) in (4) when the channel becomes more irregular. A smaller distance step for an explicit scheme, and consequently a smaller time step, is often needed to provide the same accuracy as the implicit scheme for these situations.

Little difference in the computational results was observed between the explicit and the implicit schemes for prismatic rectangular channels. It is, therefore, desirable to use the explicit scheme in situations where the implicit scheme does not provide reliable accuracy, such as the near critical mixed flows, while the other reaches are routed by the implicit scheme. In this way, one can take advantage of both schemes.

In the FLDWAV model, the implicit-explicit multiple dynamic routing algorithm is developed, and options allow the user to select a different scheme for any subreach within the entire routing reach. The upwind, explicit algorithm, when combined with the four-point implicit scheme, enables only those portions of an entire river system being modeled to use the advantages of accuracy and stability of an explicit method for nearly critical flows, while minimizing the effect of its greater computational requirement by using the implicit algorithm for other reaches of the river system where nearly critical flows do not occur.

Fig. 6 is a schematic illustration of the multiple dynamic-routing capability within the FLDWAV model. The explicit scheme is used for a subreach from x_a to x_b, and the four-point implicit scheme is used for a subreach from x_b to x_c. The time step (from t^n to t^{n+1}) for the implicit scheme is Δt_I, and the explicit scheme has a smaller time step, Δt_E, as shown in Fig. 6. The explicit subreach will have several computational time steps for one implicit time step because of the Courant condition restricting the size of a stable time step. The entire reach is thus split into two subreaches, and each subreach is computed separately. The upstream subreach is computed first, and a computed loop-rating curve is used as the downstream boundary condition for the first routing subreach. The use of the loop-rating boundary condition assumes that a free-flow

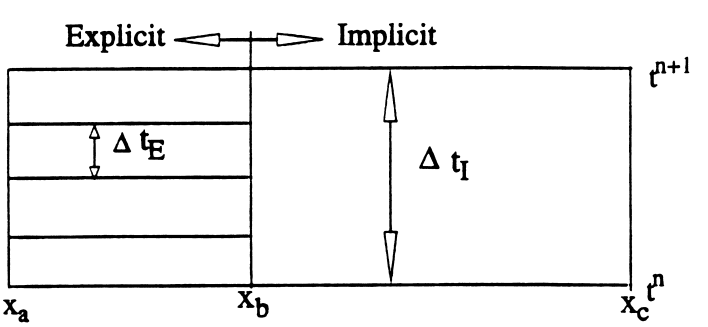

FIG. 6. Implicit-Explicit Multiple Routing

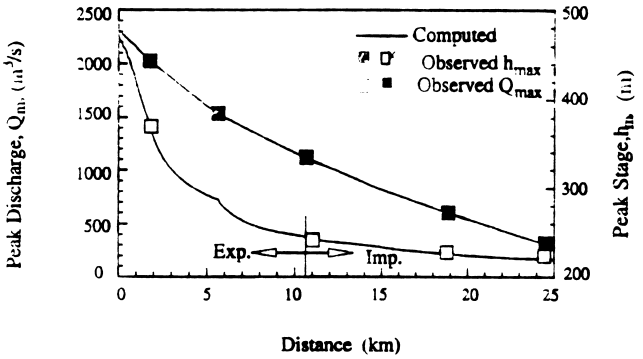

(a)

FIG. 7(a). Profiles of Peak Flows for Buffalo Creek Dam

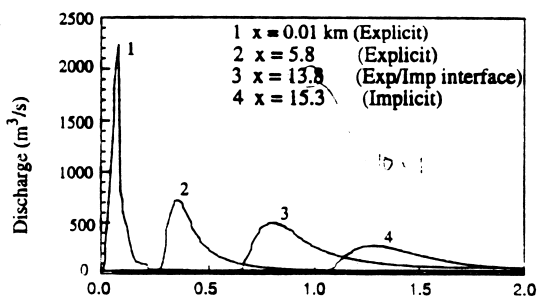

(b)

FIG. 7(b). Discharge Hydrographs for Buffalo Creek Dam

condition exists with no backwater effects, but it does account for the unsteady (dynamic) effects neglected by single-value ratings. The connecting cross section in this multiple routing, therefore, must be located where the channel shape has little change, and the backwater effects from any downstream dam, bridge, or other cross-sectional constriction are insignificant. The first routing subreach is computed for one implicit time step, and the downstream subreach can be computed using the computed discharge from the first subreach as its upstream boundary condition. Also, the implicit scheme may be used in an upstream subreach and the explicit scheme used in the downstream subreach. An entire routing reach can be divided into various implicit-explicit or explicit-implicit combinations.

The implicit-explicit multiple dynamic routing capability is a part of a general multiple-routing technique developed in the FLDWAV model, which can combine dynamic-routing methods (implicit, explicit) or hydrologic-routing methods (level pool, Muskingum-Cunge).

Figs. 7(a) and 7(b) are some results of an application of the multiple-routing technique to an actual dam-break problem—the Buffalo Creek coal-waste dam that collapsed in February 1972, on the Middle Fork, a tributary of Buffalo Creek in West Virginia. Observations (Davies et al. 1972) were available on the approximate development sequence of the breach, the time required to empty the reservoir, indirect peak discharge measurements at four sites, approximate flood-peak travel times, and flood-peak elevations. Also, nonprismatic cross sections and the Manning roughness coefficients were taken from a report on routing dam-break floods (McQuivey and Keefer 1975). The computational results are excellent compared with the observed data, e.g., the average error for the peak elevation is about 0.24 m. Some nonuniformity in the computed peak discharge profile at about $x = 5.8$ km is associated with a large change in the channel slope at that location.

In this application, level-pool (upstream of the dam at 0.0 km), explicit (0.0–10.9 km), and implicit (10.9 to 25.3 km) multiple routing is used. The breach parameters used to generate the reservoir outflow are time of failure of 0.083 h; trapezoidal-shaped breach side slope of 2.6; breach bottom width of 52 m; and breach height of 13.4 m. Distance steps are gradually increased from 0.08 km near the dam to 1.29 km downstream, and time steps are 0.004 h for the implicit and level-pool solutions, and 0.001 h for the explicit solution. The 25.3 km routing reach has two distinct subreaches with the slope changing at 5.79 km from about 0.0159 upstream to 0.0076 downstream. The resulting unsteady flow has a mixed flow regime changing from supercritical in the upstream reach to subcritical in the downstream reach.

CONCLUSION

A characteristics-based, upwind, explicit scheme is introduced for the numerical solution of 1D unsteady flows in natural rivers. It has been found that this explicit scheme has advantages over a four-point implicit scheme with a mixed flow technique for some special unsteady flow situations having moving subcritical/supercritical interfaces and subcritical/supercritical mixed-flow regimes at the near critical flow range.

The new characteristics-based, upwind, explicit scheme is implemented within the NWS FLDWAV model so that it provides an alternative numerical solution scheme for the Saint Venant equations applied to natural rivers with nonprismatic cross sections, off-channel storage, cross sections with a flood plain, and various internal boundary conditions. A technique of implicit-explicit multiple routing, within an application of the NWS FLDWAV model, is developed to take advantage of the two different schemes. The addition of the upwind, explicit scheme increases the capability and improves the performance for some special unsteady mixed-flow applications of the FLDWAV model.

APPENDIX I. REFERENCES

Chow, V. T., Maidment, D. R., and Mays, L. W. (1988). *Applied hydrology*. McGraw-Hill Book Co., Inc., New York, N.Y.

Davies, W. E., Bailey, J. F., and Kelly, D. B. (1972). "West Virginia's Buffalo Creek flood: a study of the hydrology and engineering geology." *Res. Rep., Geological Survey Circular 667*, U.S. Geological Survey.

Fennema, R. J., and Chaudhry, M. H. (1986). "Explicit numerical schemes for unsteady free-surface flows with shocks." *Water Resour. Res.*, 32(13), 1923–1930.

Fennema, R. J., and Chaudhry, M. F. (1987). "Simulation of one-dimensional dam-break flows." *J. Hydr. Res.*, 25(1), 41–51.

Fread, D. L. (1971). "Discussion of 'Implicit flood routing in natural channels,' by M. Amein and C. S. Fang." *J. Hydr. Engrg.*, ASCE, 97(7), 1156–1159.

Fread, D. L. (1977). "The development and testing of a dam-break flood forecasting model." *Proc., Dam-Break Flood Modeling Workshop*, U.S. Water Resources Council, Washington, D.C., 1–32.

Fread, D. L. (1978). "NWS operational dynamic wave model, verification of mathematical and physical models in hydraulic engineering." *Proc., 26th Annu. Hydr. Div. Spec. Conf.*, College Park, Md., 455–464.

Fread, D. L. (1983). "Computational extensions to implicit routing models." *Proc. of the Conf. on Frontiers in Hydr. Engrg.*, ASCE, New York, N.Y., 343–348.

Fread, D. L. (1985). "Channel routing." *Hydrological forecasting*, M. G. Anderson and T. P. Burt, eds., John Wiley & Sons, Inc., New York, N.Y., 437–503.

Fread, D. L. (1988). "The NWS DAMBRK model: theoretical background and user documentation." *HRL-258*, Hydrologic Research Laboratory, National Weather Service, Silver Spring, Md.

Fread, D. L. (1993). "Flood routing." *Handbook of hydrology*, D. R. Maidment, ed., McGraw-Hill Book Co., Inc., New York, N.Y., 10.1–10.36.

Fread, D. L., and Jin, M. (1993). "Real-time dynamic flood routing with NWS FLDWAV model using Kalman filter updating." *Engineering hydrology*, Y. K. Chin, ed., ASCE, New York, N.Y., 946–951.

Fread, D. L., and Lewis, J. M. (1993). "Selection of Δx and Δt at com-

putational steps for four-point implicit nonlinear dynamic routing models." *Hydraulic engineering '93*, H. W. Shen, S. T. Su, and F. Wen, eds., ASCE, New York, N.Y., 1569–1573.
Jha, A. K., Akiyama, J., and Ura, M. (1995). "First- and second-order flux difference splitting schemes for dam-break problem." *J. Hydr. Engrg.*, ASCE, 121(12), 877–884.
McQuivey, R. S., and Keefer, T. N. (1975). "Application of simple dam break routing model." *Proc. of 16th Congr. of IAHR*, IAHR, Vol. 2, 315–324.
Nakatani, T., and Komura, S. (1993). "A numerical simulation of flow with hydraulic jump using TVD-McCormack scheme." *Proc., XXV Congr. of IAHR*, IAHR, Vol. 1, 9–13.
Savic, L. J., and Holly, F. M. Jr. (1993). "Dambreak flood waves computed by modified Godunov method." *J. Hydr. Res.*, 31(2), 187–204.
Stoker, J. J. (1957). *Water waves*. Interscience Pub. Inc., New York, N.Y.
Yang, J. Y., Hsu, C. A., and Chang, S. H. (1993). "Computations of free surface flows." *J. Hydr. Res.*, 31(1), 20–33.

APPENDIX II. NOTATION

The following symbols are used in this paper:

A = active cross-sectional area of channel;
A_o = inactive (off-channel) cross-sectional area;
B = wetted top width of cross section;
C_b = bulk wave speed;
C_n = Courant number;
C_w = nondimensional wind coefficient;
c = local dynamic wave velocity;
g = gravity constant;
h = water-surface elevation (stage);
h_b = elevation of channel bed;
K_c = channel conveyance factor;
K_e = expansion or contraction coefficient;
L = momentum effect of lateral flow;
M = constant;
n = Manning's resistance coefficient;
P_1 = state variable integral function term in Eq. (7);
P_2 = state variable integral function term in Eq. (7);
Q = discharge;
q = later inflow or outflow;
R = hydraulic radius;
S_e = local loss slope;
S_f = friction slope due to bed resistance;
T_f = time of failure of dam;
T_r = hydrograph's time of rise;
t = time;
V_r = speed of wind relative to velocity of channel flow;
V_w = speed of wind;
v = local cross-sectional average velocity;
w = azimuth angle of wind to x-axis;
x = distance along longitudinal axis of channel;
Δt = computational time interval;
Δx = computational distance step; and
λ = system of units coefficient in Manning equation.